The EMBO Journal (2013) 32, 1927–1940
www.embojournal.org

OPEN ACCESS TRANSPARENT PROCESS

THE EMBO JOURNAL

OPA1 promotes pH flashes that spread between contiguous mitochondria without matrix protein exchange

Jaime Santo-Domingo[1], Marta Giacomello[1], Damon Poburko[2], Luca Scorrano[1] and Nicolas Demaurex[1,*]

[1]Department of Cell Physiology and Metabolism, University of Geneva, Geneva, Switzerland and [2]Department of Biomedical Physiology and Kinesiology, Simon Fraser University, Burnaby, British Columbia, Canada

The chemical nature and functional significance of mitochondrial flashes associated with fluctuations in mitochondrial membrane potential is unclear. Using a ratiometric pH probe insensitive to superoxide, we show that flashes reflect matrix alkalinization transients of ~0.4 pH units that persist in cells permeabilized in ion-free solutions and can be evoked by imposed mitochondrial depolarization. Ablation of the pro-fusion protein Optic atrophy 1 specifically abrogated pH flashes and reduced the propagation of matrix photoactivated GFP (paGFP). Ablation or invalidation of the pro-fission Dynamin-related protein 1 greatly enhanced flash propagation between contiguous mitochondria but marginally increased paGFP matrix diffusion, indicating that flashes propagate without matrix content exchange. The pH flashes were associated with synchronous depolarization and hyperpolarization events that promoted the membrane potential equilibration of juxtaposed mitochondria. We propose that flashes are energy conservation events triggered by the opening of a fusion pore between two contiguous mitochondria of different membrane potentials, propagating without matrix fusion to equilibrate the energetic state of connected mitochondria.

The EMBO Journal (2013) **32,** 1927–1940. doi:10.1038/emboj.2013.124; Published online 28 May 2013
Subject Categories: membranes & transport
Keywords: bioenergetics; cell signalling; metabolism

Introduction

Mitochondria are double-membrane organelles that play a central role in cellular energy conversion, lipid metabolism, calcium signalling, and apoptosis. The generation of ATP by oxidative phosphorylation involves the generation of a proton-motive force (Δp) across the inner mitochondrial membrane (IMM) as protons are pumped by respiratory chain complexes and subsequently used to drive the activity of the ATP synthase. Δp comprises an electrical component, the mitochondrial membrane potential ($\Delta\Psi_m$ ~180 mV, negative inside), and a chemical component, the transmembrane pH gradient (ΔpH_m ~0.8, alkaline inside), whose generation is facilitated by the low H^+-buffering capacity of the alkaline mitochondrial matrix (Poburko *et al*, 2011). While some electrogenic transporters are driven exclusively by $\Delta\Psi_m$, the transport of many ions, substrates, and metabolites depends on ΔpH_m (Bernardi, 1999).

Improvements in live cell fluorescence imaging have revealed that $\Delta\Psi_m$ fluctuates rapidly within individual mitochondria and that these electrical events can propagate along interconnected mitochondria (Duchen *et al*, 1998; Huser *et al*, 1998; Huser and Blatter, 1999; De Giorgi *et al*, 2000). A plethora of mechanisms were proposed to trigger the $\Delta\Psi_m$ fluctuations: local Ca^{2+} elevations (Duchen *et al*, 1998), opening of the mitochondrial permeability transition pore (mPTP) (Huser and Blatter, 1999; De Giorgi *et al*, 2000; Zorov *et al*, 2000; Jacobson and Duchen, 2002), coupling of $\Delta\Psi_m$ to the ATP synthase (Thiffault and Bennett, 2005), switching between active and inactive states of oxidative phosphorylation (Buckman and Reynolds, 2001), or opening of a proton-selective channel by matrix alkalinization (Hattori *et al*, 2005). Spontaneous $\Delta\Psi_m$ fluctuations are also observed in permeabilized cells (Uechi *et al*, 2006) and in isolated mitochondria, where they are modulated by adenine nucleotides acting from the matrix side (Vergun *et al*, 2003; Vergun and Reynolds, 2004). In astrocytes, spontaneous $\Delta\Psi_m$ decreases are associated with transient elevations in matrix $[Na^+]$ (Azarias *et al*, 2008), whereas in cardiac myocytes synchronized $\Delta\Psi_m$, reactive oxygen species (ROS), and NADP fluctuations were reported and attributed to the opening of a mitochondrial anion channel permeable to superoxide (Aon *et al*, 2003). In skeletal muscle cells and intact beating hearts, superoxide flashes coinciding with $\Delta\Psi_m$ decreases were recorded with a circularly permutated yellow fluorescent protein (cpYFP) and proposed to be generated by stochastic openings of the mPTP that, by dissipating $\Delta\Psi_m$, divert electrons from the respiratory chain to generate bursts of matrix superoxide (Wang *et al*, 2008). Subsequent studies using cpYFP-based probes indicated that flash frequency is linked to mitochondrial respiration (Pouvreau, 2010; Wei *et al*, 2011) and increases during oxidative stress-induced apoptosis (Ma *et al*, 2011), reviewed in Fang *et al* (2011). The superoxide nature of the flashes is disputed, however (Muller, 2009), and because cpYFP is also pH sensitive (Nagai *et al*, 2001) several groups have instead proposed that the flashes are transient mitochondrial matrix pH (pH_{mito}) elevations (Azarias and Chatton, 2011; Schwarzlander *et al*, 2011, 2012a), reviewed in Santo-Domingo and Demaurex (2012) and Schwarzlander *et al* (2012b).

*Corresponding author. Department of Cell Physiology and Metabolism, University of Geneva, 1, rue Michel-Servet, Geneva 4 CH-1211, Switzerland. Tel.: +41 22 379 5399; Fax: +41 22 379 5338; E-mail: Nicolas.Demaurex@unige.ch

Received: 12 October 2012; accepted: 19 April 2013; published online: 28 May 2013

Energy conservation across the IMM depends on its impermeability to protons; however, the maintenance of this permeability barrier is challenged in intact cells by the understanding that mitochondria are not isolated organelles and that they undergo cycles of fission and most importantly fusion (Twig *et al*, 2008). Mitochondrial fission depends on the cytoplasmic dynamin-related protein 1 (DRP1) (Smirnova *et al*, 2001), that is recruited on the organelle by several potential receptors like FIS1, MFF, and MID49/51 (Palmer *et al*, 2011). Fusion depends on the outer mitochondrial membrane (OMM) proteins Mitofusin (MFN) 1 and 2 and on the IMM Optic atrophy 1 (OPA1) (Campello and Scorrano, 2010). Mitochondrial fusion is a complex process from the membrane biology and the bioenergetic point of view: fusion of two organelles involves the generation of a fusion intermediate of four membranes; if the process of mitochondrial fusion is analogous to other organellar fusions, when the IMM fuses a fusion pore shall be generated that would link two matrixes. Such a fusion pore might connect two mitochondria of different respiratory states, with unpredictable effects on their membrane potential. Defective fusion pore assembly could even connect the matrix with the intermembrane space. *In vitro* experiments indicate that OPA1 induces lipid tubulation (Ban *et al*, 2010), and rupture of the growing IMM tubules could link the matrix to the IMS. If pore formation involves the juxtaposition of two hemichannels as for gap junctions, opening of the hemichannels on the growing IMM tubule would also connect the matrix to the IMS, equilibrating two chemically different environments with profound consequences on the bioenergetics of the organelle.

Here we set out to address, by combining genetics and physiology, how mitochondrial fusion impacts on bioenergetics. Our ratiometric probe SypHer, highly pH-sensitive but insensitive to superoxide *in vitro*, recorded changes in matrix pH in single mitochondria. Spontaneous alkalinization transients coincided with decreases in $\Delta\Psi_m$. We could unravel that these flashes represented compensatory pH_{mito} elevations maintaining the proton-motive force during spontaneous decreases in $\Delta\Psi_m$. In cells lacking OPA1, the flashes were completely absent, whereas their propagation was greatly increased when mitochondria were more interconnected. A significant fraction of adjacent mitochondria exhibited opposite changes in $\Delta\Psi_m$ during pH_{mito} flashes that resulted in membrane potential equilibration. We propose that the pH_{mito} flashes are energy conservation events requiring the fusion protein OPA1 and therefore triggered by the opening of fusion pores between adjacent mitochondria. The flashes propagate without matrix mixing between adjacent mitochondria, a new mode of coupling that might allow interconnected mitochondria to rapidly equilibrate their energetic state.

Results

Spontaneous alkalinization transients in single mitochondria

We recently generated a new pH-sensitive probe targeted to the matrix of mitochondria, mito-SypHer, and reported dynamic changes in the mitochondrial pH gradient in HeLa cells (Poburko *et al*, 2011). During these recordings, we frequently observed spontaneous and asynchronous increases in mito-SypHer ratio fluorescence in discrete regions of the mitochondrial network (Figure 1 and Supplementary Movie S1). The elevations occurred either in different regions of the cell (Figure 1A) or repeatedly at the same location (Figure 1B), but always remained restricted to a specific region of the mitochondrial network (Figure 1B, inset). The elevations had an abrupt onset (time to peak: 1.63 ± 0.08 s) followed by a slower recovery towards basal levels, and a mean life time of 8.6 ± 0.6 s (Figure 1C–E). On average, 0.54 ± 0.04 elevations were detected per minute per cell. *In situ* pH calibration of the probe by titration with buffers of different pH in the presence of the K^+/H^+ ionophore nigericin (Supplementary Figure S1) revealed that the matrix pH increased by 0.38 ± 0.04 pH units during a typical event, from 7.75 ± 0.21 to 8.14 ± 0.46 (Figure 1D and E). Transient alkalinization events of sizable magnitude thus occur in intact mitochondria.

cpYFP flash activity has been shown to require an active respiratory chain (Wang *et al*, 2008; Schwarzlander *et al*, 2012a). Accordingly, inhibition of complex I, III, IV, and V with rotenone, antimycin, azide, and oligomycin, respectively, decreased the frequency of SypHer flashes (Figure 2A–D). Furthermore, *Rho 0* cells, which lack mtDNA and thus all H^+-translocating complexes, lacked pH_{mito} activity (Figure 2A, inset). The strongest inhibitors were antimycin and the protonophore carbonyl cyanide m-chlorophenyl hydrazone (CCCP) (Figure 2A), at doses increasing respiration (Supplementary Figure S2C), which both collapsed ΔpH_m (Figure 2C and F). Earlier studies have linked $\Delta\Psi_m$ fluctuations to cytosolic Ca^{2+} elevations (Duchen *et al*, 1998; Vergun and Reynolds, 2004; Guzman *et al*, 2010). We could not detect mitochondrial Ca^{2+} elevations with Rhod2 during pH_{mito} flashes (Figure 2G) and neither intracellular Ca^{2+} stores depletion with thapsigargin, cytosolic Ca^{2+} buffering with (1,2-bis(*o*-aminophenoxy) ethane-N,N,N′,N′-tetraacetic acid) aceto-methyl ester (BAPTA-AM) (Figure 2H), nor genetic manipulation of the recently identified mitochondrial H^+/Ca^{2+} exchanger protein Letm1 (Supplementary Figure S2) had any impact on flash activity. This indicates that pH_{mito} flashes are not driven by mitochondrial Ca^{2+} uptake. $\Delta\Psi_m$ fluctuations were attributed to mPTP opening by ROS (Huser and Blatter, 1999; Jacobson and Duchen, 2002; Wang *et al*, 2008). In our hands, mPTP inhibitors (cyclosporine A and bongkrekic acid) and ROS scavengers (Tyron and Tocopherol) did not significantly alter pH_{mito} flash frequency (Figure 2I), indicating that flash activity is not driven by mPTP opening, although atractyloside increased flash frequency by $\sim$5-fold.

Mito-SypHer is a specific pH indicator insensitive to superoxide

The pH_{mito} elevations reported by the ratiometric mito-SypHer probe resemble the superoxide and pH_{mito} flashes previously reported with cpYFP (Wang *et al*, 2008; Schwarzlander *et al*, 2012a). To clarify the chemical nature of the flashes, we evaluated the pH and superoxide sensitivity of bacterially expressed 6$\times$ His-tag SypHer. The excitation spectra of purified SypHer was highly sensitive to changes in pH (Figure 3A) but was not affected by the addition of xanthine and xanthine oxidase (XO) at concentrations that evoked a robust superoxide dismutase (SOD)-sensitive increase in the luminescence of the superoxide probe

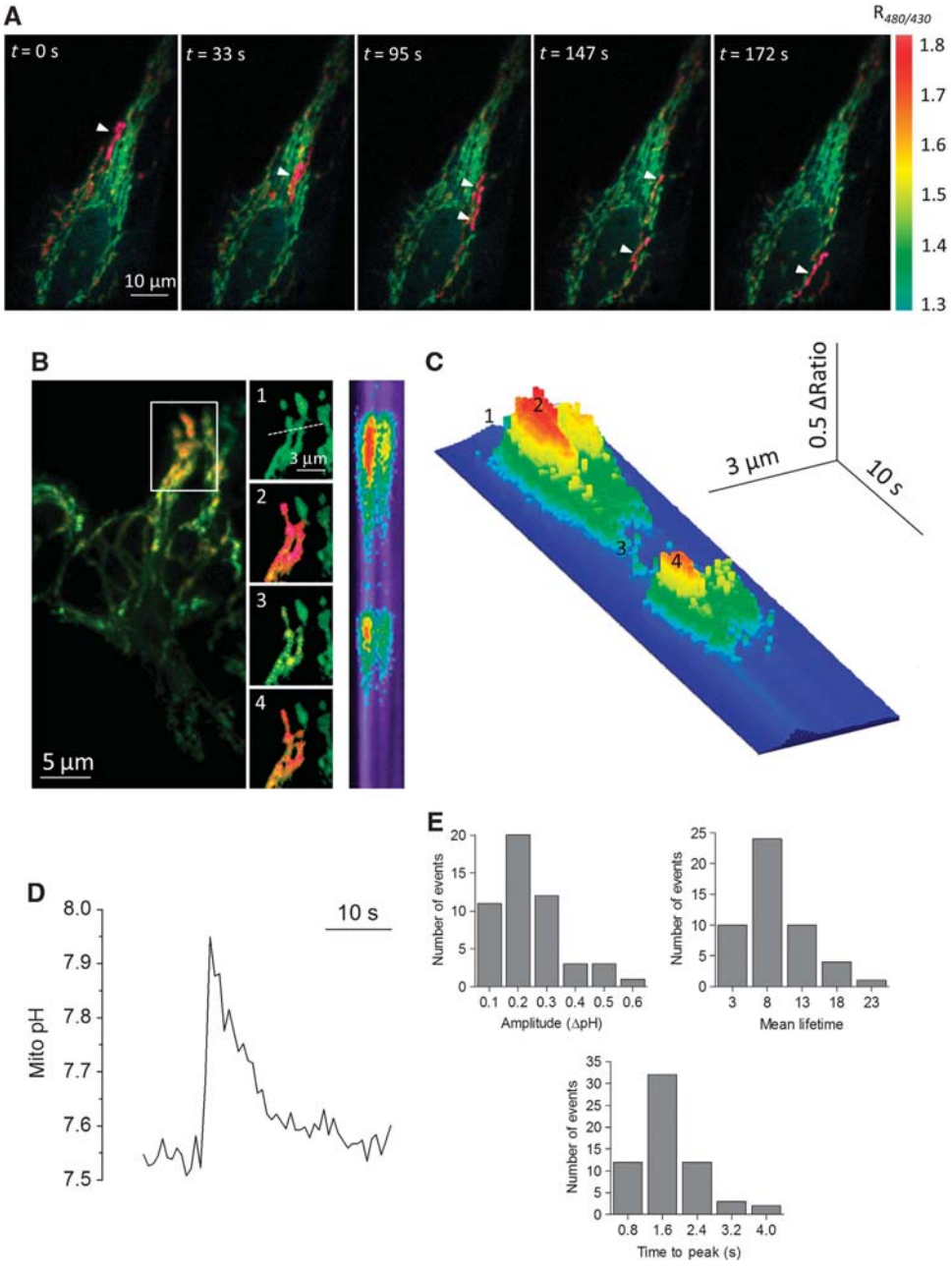

Figure 1 Transients pH_{mito} elevations in single mitochondria. (**A**) Time sequence of F480/F430 ratio images of HeLa cells expressing mito-SypHer showing spontaneous alkalinization transients (arrows) in single mitochondria in different cellular regions. Warm colours denote high ratio values. See also Supplementary Movie S1. (**B**) Repetitive pH transients in a mitochondrial cluster. Numbered insets show consecutive images and the right-hand panel shows a 30 s scan along the line drawn in inset #1, the time axis running vertically from top to bottom. (**C**) 3D reconstruction of the line scan image. Numbers correspond to inset panels in **B**. (**D**) Calibrated pH_{mito} transient. (**E**) Histograms showing the distribution of the amplitude, time to peak, and half-life time of 61 independent pH_{mito} elevations.

2-methyl-6-(*p*-methoxyphenyl)-3,7-dihydroimidazo[1,2-alpha]-pyrazin-3-one (MCLA) (Figure 3B and Supplementary Figure S3A). Furthermore, the excitation spectra of purified SypHer were not affected by H_2O_2 (Figure 3C), by the NO donor *S*-nitroso-*N*-acetyl-DL-penicillamine (SNAP), by the reducing agent dithiothreitol (DTT), or by millimolar concentrations of Ca^{2+}, PO_4^{-}, and ATP (Supplementary Figure S3B–E and Poburko *et al*, 2011). These *in vitro* data indicate that the fluorescence of mito-SypHer is insensitive to changes in redox state, ionic strength, and metabolites, and further validate the probe as a ratiometric pH indicator. Ratiometric pericam targeted to the mitochondria (RP_{mit}) reportedly responds to superoxide at 488 nm (Pouvreau, 2010), but this indicator is not specific for superoxide as its fluorescence increases sharply above pH 7.0 (Figure 3D, inset) suggesting that the fluorescence flashes reported by RP_{mit} in HeLa cells (Figure 3D) also reflect an increase in matrix pH. Next, we increased the proton-buffering power of mitochondria with the permeable weak base NH_4Cl, a procedure expected to alter the kinetics of proton but not of superoxide changes. Since NH_4Cl increases pH_{mito}, the fluorescence data were converted to proton concentrations and expressed in a non-logarithmic scale to compare the absolute changes in $[H^+]$ (Figure 2E). Both the onset and the recovery of the $[H^+]$

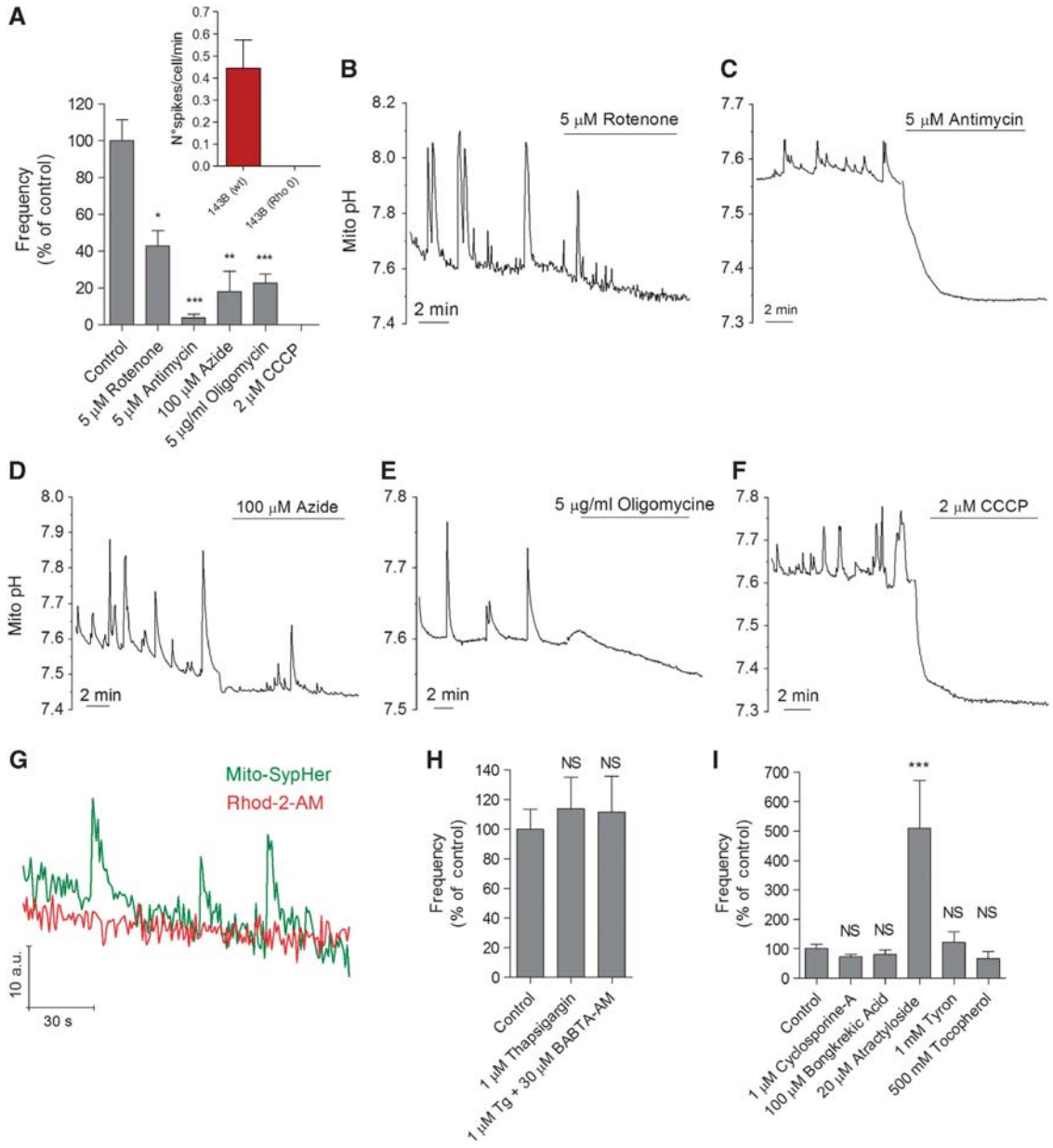

Figure 2 Pharmacology of pH_{mito} flashes. (**A**) Effect of respiratory chain inhibitors on the frequency of pH_{mito} flashes in 15 min recordings of 82 (control), 10 (rotenone), 28 (antimycin), 13 (azide), 48 (oligomycin), and 11 cells (CCCP). Inset: pH_{mito} elevations in control ($n = 14$) and mitochondria-deficient *rho 0* osteosarcoma 143b cells ($n = 12$). (**B–F**) Representative recordings of HeLa cells expressing DRP1 (K38A), showing the effect of different respiratory chain inhibitors on pH_{mito} flashes and on the basal mitochondrial pH. (**G**) Simultaneous mito-SypHer and Rhod-2 recordings. No $[Ca^{2+}]_{mito}$ changes were observed during pH_{mito} flashes. (**H**) Effect of Ca^{2+} depletion and Ca^{2+} buffering on the frequency of pH_{mito} flashes. Cells were treated with thapsigargin (Tg) to deplete Ca^{2+} stores and subsequently loaded with BAPTA-AM to chelate cytosolic Ca^{2+} ($n = 26$, 21, and 14 cells). (**I**) Effect of mPTP modulators on the frequency of pH_{mito} flashes ($n = 9$–44 cells, means ± s.e.m.). $^{*}P < 0.05$, $^{**}P < 0.01$, and $^{***}P < 0.001$. NS, not significant.

transients were delayed in the presence of the weak base, and their amplitude decreased by 82% (Figure 3E, $n = 49$–59). Thus, increasing the buffering power of mitochondria decreased the amplitude and prolonged the duration of the spontaneous transients, providing independent functional evidence that the SypHer flashes are caused by protons and not by superoxide.

pH_{mito} flashes are bioenergetic events driven by decreases in $\Delta\Psi_m$

We next recorded pH_{mito} in cells permeabilized with digitonin and perfused with succinate. pH_{mito} flashes were readily observed in permeabilized cells (Figure 4A, inset), a configuration that, as shown previously (Poburko *et al*, 2011), allowed basal pH_{mito} levels to vary rapidly and reversibly with the cytosolic pH (Supplementary Figure S4A). Succinate removal reduced flash frequency by 93%, whereas substitution of Na^+, K^+, Ca^{2+}, Cl^-, and PO_4^{2-} with sucrose increased flash frequency without altering their kinetics or amplitude. Decreasing cytosolic pH from 7.5 to 7.0 did not significantly decrease flash frequency, but further acidification to pH 6.5 decreased flash frequency by ~50% (Figure 4A). The pH_{mito} flashes thus persisted in permeabilized cells, their frequency increasing in ion-free conditions

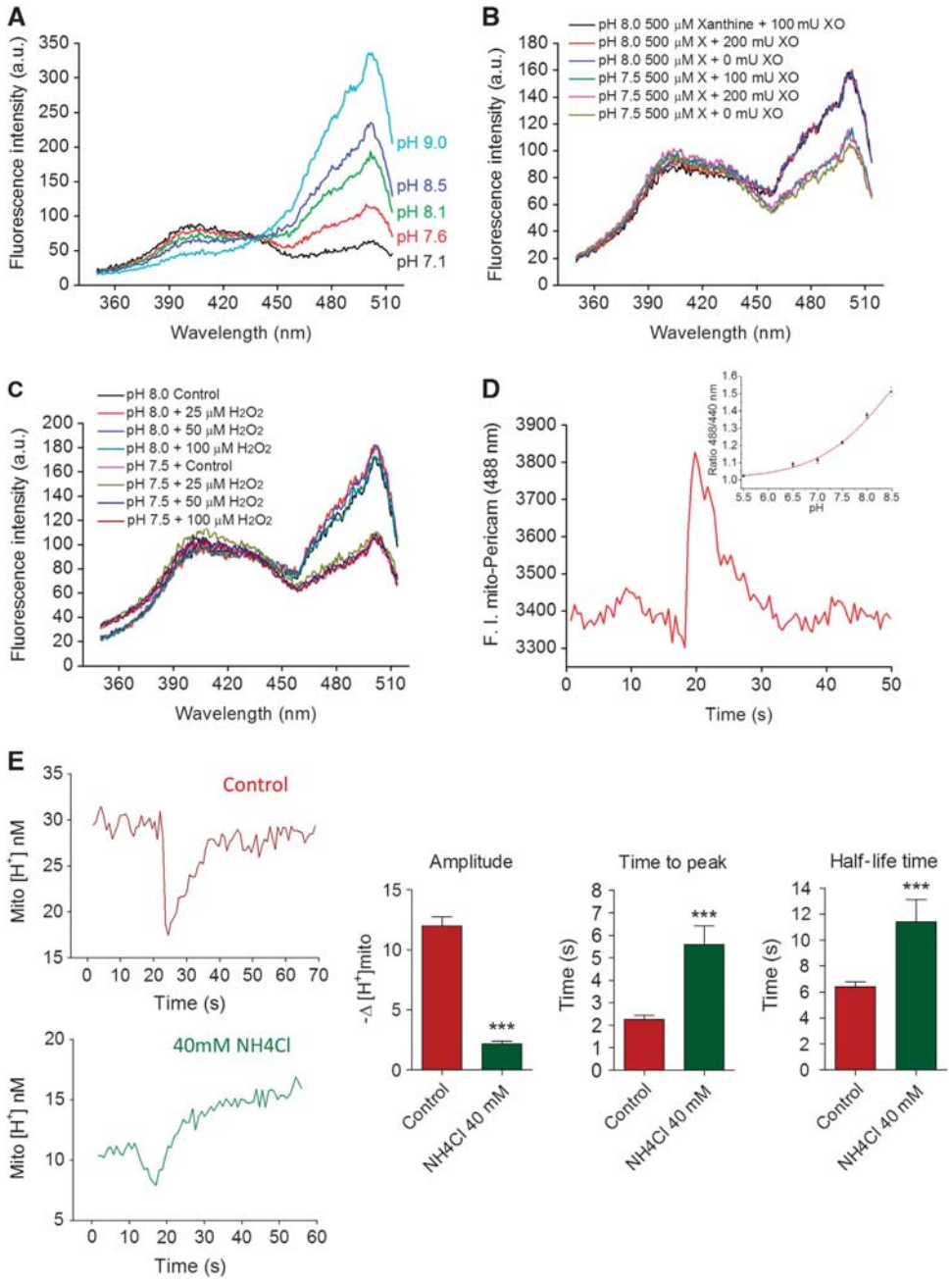

Figure 3 Mito-SypHer is a pH-sensitive probe insensitive to superoxide. (**A**) Excitation spectra ($\lambda_{em} = 530$ nm) of purified bacterially expressed SypHer at different pH. (**B**) Excitation spectra of purified SypHer in the presence of xanthine and XO at pH 7.5 and pH 8.0. (**C**) Excitation spectra in the presence of increasing amounts of H_2O_2. Spectra are representative of three independent experiments in each condition. (**D**) Spontaneous fluorescence elevations recorded with ratiometric pericam (RP_{mit}, $\lambda_{em} = 488$ nm) in HeLa cell mitochondria. ($n = 52$ transients from three cells). Inset: effect of pH on RP_{mit} F488/F440 ratio fluorescence. (**E**) Effect of 40 mM NH_4Cl on the kinetics and amplitude of the pH_{mito} elevations recorded with SypHer. Left panels: the fluorescence recordings were converted to proton concentrations and expressed in a non-logarithmic scale to compare the absolute changes in $[H^+]$. Right panels: averaged amplitude, time to peak, and half-life time of 56 pH_{mito} elevations recorded in six cells before (red) and after (green) addition of 40 mM NH_4Cl (means ± s.e.m.). $^{***}P < 0.001$.

and decreasing under acidic conditions and substrate removal. These data indicate that the pH_{mito} flashes are not driven by the entry of ions into mitochondria, and that the flash activity requires respiring mitochondria and a permissive matrix or cytosolic pH but not cytosolic ions.

The cpYFP flashes occur coincidentally with decreases in $\Delta\Psi_m$ (Wang *et al*, 2008). We also observed a concomitant decrease in $\Delta\Psi_m$ with every pH_{mito} elevation during simultaneous SypHer and tetramethyl rhodamine methyl ester (TMRM) recordings (Figures 4B–C, $n = 64$ events, Supplementary movie S2). In most cases (96%), the depolarization events were transient and mirrored the pH_{mito} elevations (Figure 4C, left traces), but on rare occasions (4%) mitochondria remained depolarized for several seconds after the termination of the pH_{mito} flash (Figure 4C, right traces). The upstroke of the pH_{mito} and $\Delta\Psi_m$ transients was faster than the temporal resolution of our imaging setup (20 Hz), and the two activities thus appeared coincidental. The mirror

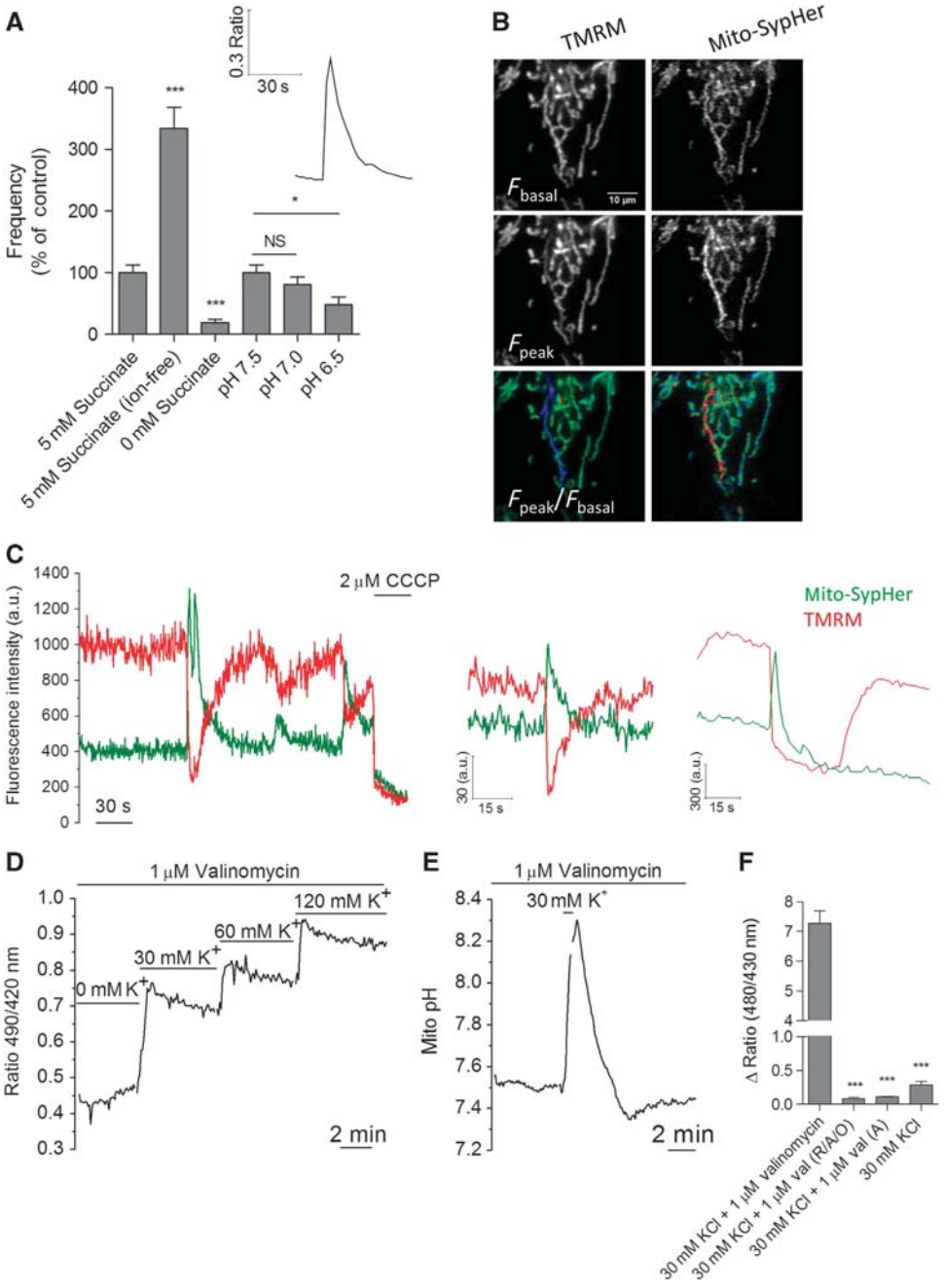

Figure 4 pH_{mito} flashes are bioenergetic events driven by decreases in $\Delta\Psi_m$. (**A**) Spontaneous elevations in mito-SypHer fluorescence in HeLa cells permeabilized in KCl-based solutions. Inset shows a typical pH_{mito} flash, bar graph shows the frequency of flashes recorded in solutions containing ($n = 64$) or lacking ions (Ca^{2+}, Na^+, K^+, and PO_4^- replaced with sucrose, $n = 62$), respiratory substrates ($n = 32$), and of varying pH ($n = 64$ for each condition) (means ± s.e.m.). (**B**) Simultaneous pH_{mito} and $\Delta\Psi_m$ recordings in intact cells loaded with TMRM. A concomitant decrease in $\Delta\Psi_m$ was observed in 64/64 flashes. See also Supplementary Movie S2. (**C**) $\Delta\Psi_m$ typically mirrored pH_{mito} (left panels) but occasionally exhibited delayed recovery (right panel). (**D**) Effect of imposed mitochondrial depolarizations on pH_{mito}. Permeabilized cells were equilibrated with valinomycin and exposed to increasing concentration of KCl to clamp $\Delta\Psi_m$ at different depolarized potentials. Increasing depolarization steps induced progressive matrix alkalinization ($n = 37$ cells). (**E**) pH_{mito} elevation evoked by a brief pulse of 30 mM KCl to transiently depolarize mitochondria ($n = 68$). (**F**) Effect of respiratory chain inhibitors and of valinomycin on the amplitude of the pH_{mito} elevation evoked by KCl. A, antimycin; O, oligomycin; R, rotenone; Val, valinomycin ($n = 50$ cells for each condition; means ± s.e.m.). $^*P < 0.05$ and $^{***}P < 0.001$. NS, not significant.

changes in $\Delta\Psi_m$ and pH_{mito} reflect opposite alterations in the electrical and chemical components of the proton-motive force, suggesting that ΔpH_m increases to balance the decrease in $\Delta\Psi_m$ (Santo-Domingo and Demaurex, 2012). To test this possibility, we clamped the $\Delta\Psi_m$ at different potentials by equilibrating permeabilized cells with valinomycin at different K^+ concentrations. As predicted, addition of 30 mM KCl evoked an immediate increase in pH_{mito}, and subsequent additions of higher K^+ concentrations further alkalinized the matrix (Figure 4D). To test whether a pH_{mito} flash could be evoked by an artificial depolarization, we briefly added 30 mM KCl to cells equilibrated with

valinomycin. This treatment faithfully reproduced pH_{mito} flashes, the pH_{mito} rapidly increasing upon KCl addition and slowly recovering upon KCl withdrawal (Figure 4F). KCl had no effect in the absence of valinomycin (Figure 4G) and pH_{mito} flashes were also evoked by addition of NaCl or LiCl to permeabilized cells treated with the ionophore A23187 (Supplementary Figure S4B), ruling out K^+/H^+ exchange. The KCl-evoked pH_{mito} elevations were prevented by respiratory chain inhibitors (Figure 4G), confirming that they reflected increases in proton pumping. Thus, pH_{mito} flashes can be artificially generated by an imposed transient mitochondrial depolarization, strongly suggesting that the endogenous flash activity of intact cells reflects compensatory increases in ΔpH driven by spontaneous decreases in $\Delta\Psi_m$. The $\Delta\Psi_m$ changes coincided both spatially and temporally with the matrix pH flashes (Figure 4B and Supplementary Figure S4C), suggesting that the electrical events propagate along connected mitochondria and trigger immediate pH responses in depolarized mitochondria.

Matrix pH elevations propagate faster than matrix GFP along connected mitochondria

The spatial dimension of the pH_{mito} elevations varied considerably, with some events restricted to single mitochondria and other occurring in large clusters of interconnected mitochondria (Figure 5AI,II). To test whether the area covered by a single pH_{mito} elevation varied with mitochondria interconnectivity, we enforced mitochondrial shape changes by overexpressing mitochondrial-shaping proteins. Elongation was promoted by a dominant-negative DRP1 mutant ($DRP1^{K38A}$)

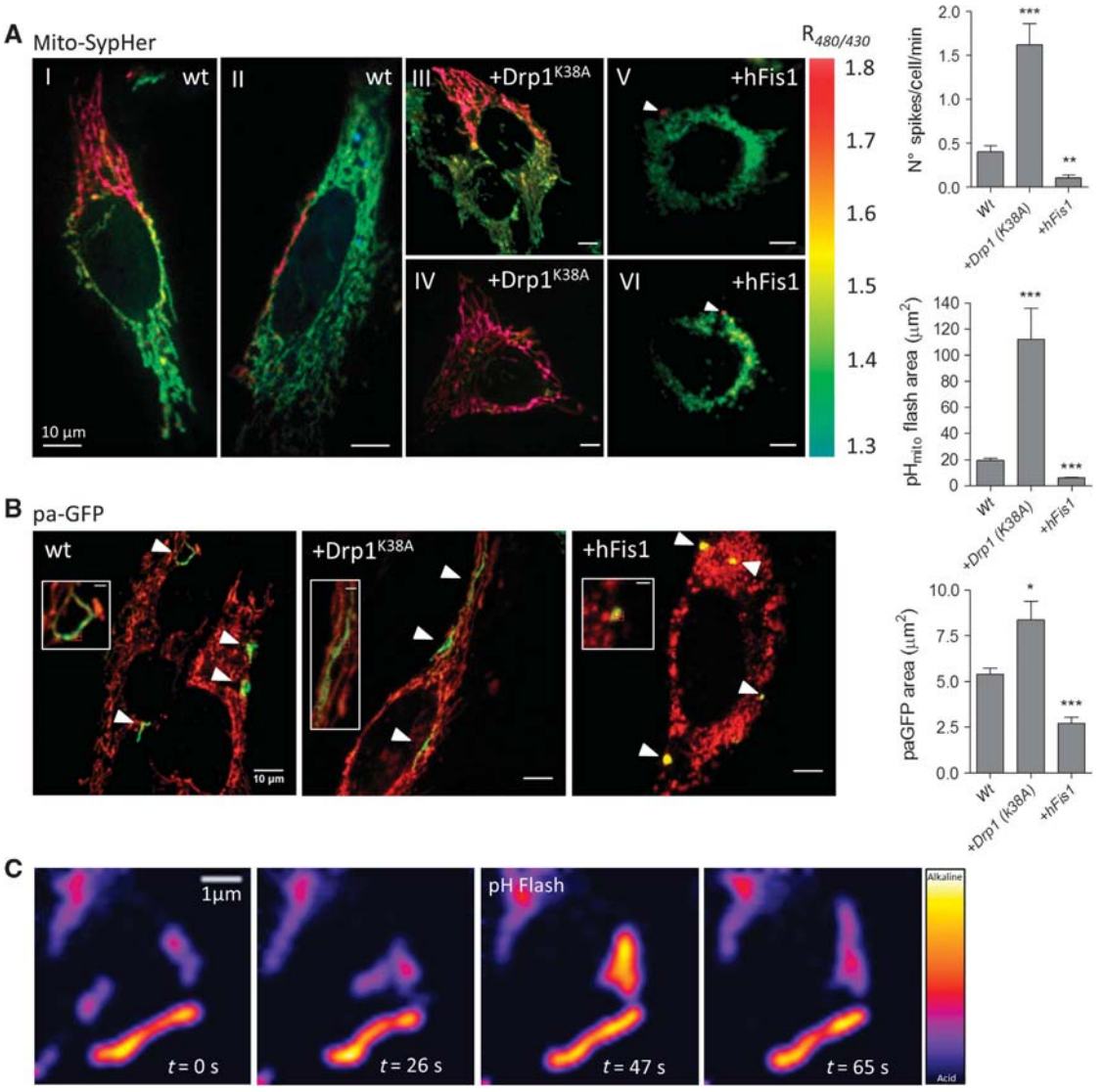

Figure 5 Matrix pH elevations propagate along connected, but not fused, mitochondria. (**A**) Ratio mito-SypHer images taken at the peak of elementary pH_{mito} elevations in WT HeLa cells (I, II) and in cells expressing the pro-fusion protein $DRP1^{K38A}$ (III, IV) or the pro-fission protein hFIS1 (V, VI). Note that in $DRP1^{K38A}$ cells pH_{mito} flashes occasionally spread over the entire mitochondrial network. See also Supplementary Movie S3. Bar graphs: averaged spatial extent and frequency of pH_{mito} flashes in 15 min continuous recordings of 11 cells for each condition (means ± s.e.m.). (**B**) Individual matrix compartments labelled with paGFP. Representative merged TMRM/paGFP fluorescence images taken 5 s after paGFP photoactivation in HeLa cells expressing the indicated plasmid; insets show paGFP-labelled regions at higher magnification, with the irradiated region indicated by a crosshair; bar graph: averaged spatial extent of matrix paGFP propagation ($n = 6$ independent experiments, means ± s.e.m.). (**C**) pH_{mito} flash occurring during transient contact between two individual mitochondria. See also Supplementary Movie S4. $^*P<0.05$, $^{**}P<0.01$, and $^{***}P<0.001$.

and fission by the pro-fission protein hFIS1 (Frieden *et al*, 2004). The spatial extension of the pH_{mito} elevations increased dramatically in cells expressing $DRP1^{K38A}$ (Figure 5AIII,IV), with global pH_{mito} flashes observed in some cells (Figure 5AIV and Supplementary movie S3), and decreased in cells expressing hFIS1 (Figure 5AV,VI). On average, a single pH_{mito} flash covered $17.02 \pm 0.32\,\mu m^2$ ($n = 81$) of the fluorescent mitochondrial area in control HeLa cells, $109.08 \pm 21.12\,\mu m^2$ ($n = 96$ flashes) in cells expressing $DRP1^{K38A}$, and only $6.41 \pm 0.08\,\mu m^2$ ($n = 59$) in hFIS1 expressers. Interestingly, the frequency of the pH_{mito} elevations increased in cells with fused mitochondria and decreased in cells with fragmented mitochondria (Figure 5A), while the flash amplitude and time to peak increased upon $DRP1^{K38A}$ and hFIS1 expression, respectively (Supplementary Figure S5A). We next tested whether flash propagation reflected luminal continuity between neighbouring organelles by measuring the matrix diffusion of a photoactivated GFP (paGFP). Photoactivation of matrix-targeted paGFP revealed areas that were much smaller than the areas of elementary

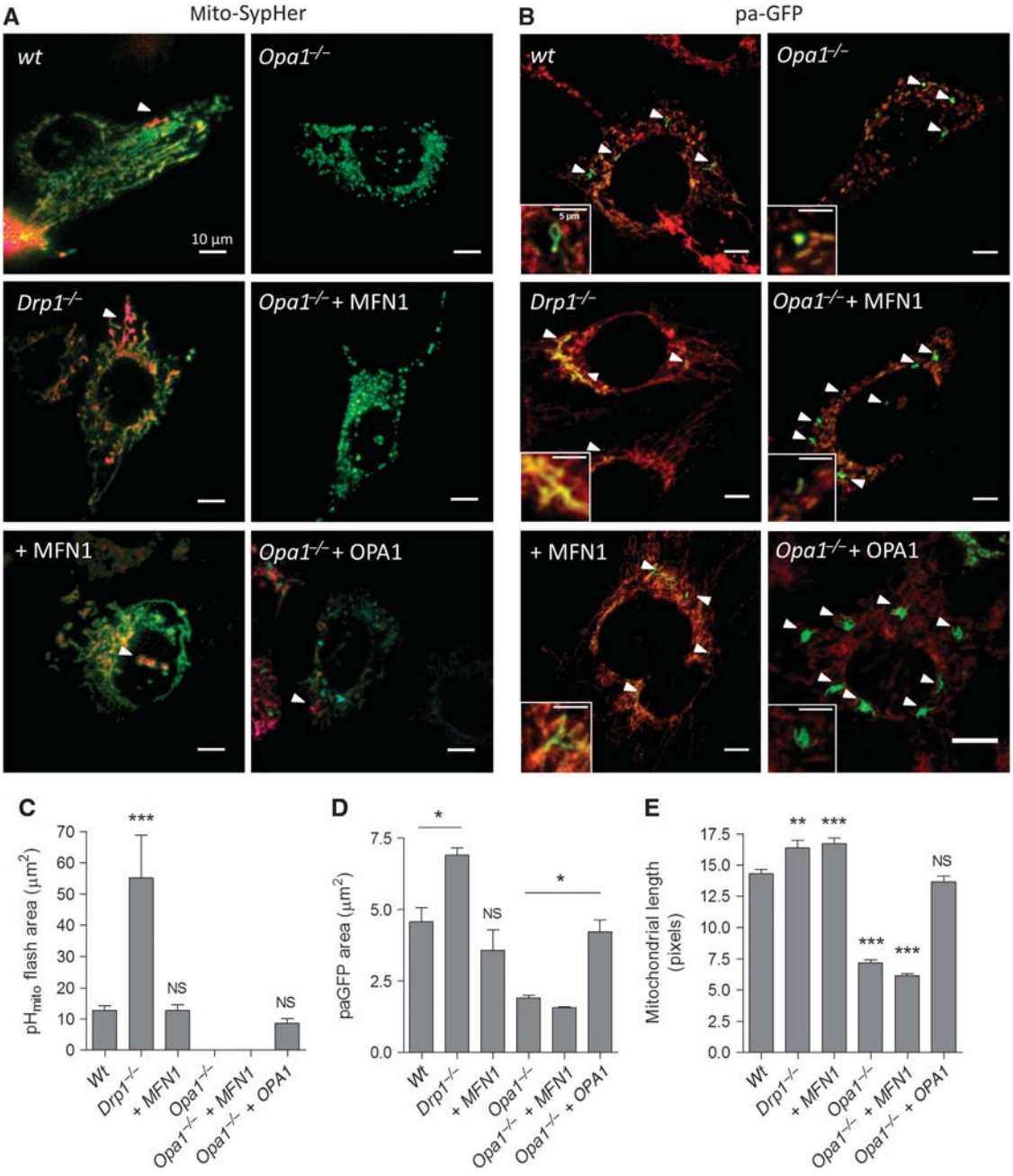

Figure 6 pH_{mito} flashes require OPA1 but not MFN1. (**A**) SypHer images taken at the peak of elementary pH_{mito} elevations in mouse embryonic fibroblasts (MEFs) derived from control, $Drp1^{-/-}$, and $Opa1^{-/-}$ mice transfected or not with MFN1 or OPA1. (**B**) Matrix compartments labelled with paGFP in cells of the indicated genotype; insets show the paGFP-labelled regions at higher magnification. Averaged spatial extent of (**C**) pH_{mito} flashes and of (**D**) paGFP propagation in 15 min continuous recordings of 30 cells for each condition ($n = 6$ independent experiments) (means ± s.e.m.). (**E**) Averaged length of individual mitochondria ($n = 300$, means ± s.e.m.). $^*P < 0.05$, $^{**}P < 0.01$, and $^{***}P < 0.001$. NS, not significant.

pH_{mito} flashes (Figure 5B, the individual matrix compartments labelled with paGFP appearing in green over the red TMRM mitochondrial staining). paGFP fluorescence covered a maximal mitochondrial area 2 s after laser illumination (Supplementary Figure S5B and C), a procedure that did not alter TMRM fluorescence (Figure 5D and E), indicating that our measurements were not limited by the rates of paGFP matrix diffusion or by laser-induced toxicity. paGFP-labelled areas were ~3-fold smaller than the pH_{mito} flash areas in non-transfected cells and ~13-fold smaller than flash area in $DRP1^{K38A}$ cells, the paGFP areas increasing by only ~30% upon $DRP1^{K38A}$ expression while the pH_{mito} flash area increased by ~6-fold (Figure 5A and B). paGFP-labelled areas of up to 47 μm^2 could be detected in $DRP1^{K38A}$ expressers, indicating that the small average size of paGFP regions did not reflect failure to detect paGFP fluorescence but rather probe confinement. Photoactivation of matrix-targeted paGFP in cells loaded with TMRM confirmed that the spontaneous $\Delta\Psi_m$ drops propagated within a much wider mitochondrial area than the matrix paGFP (data not shown). These data indicate that pH_{mito} flashes can propagate along interconnected mitochondria that have limited exchange of matrix protein content. Nevertheless, pH_{mito} and $\Delta\Psi_m$ flashes correlated temporally with mitochondrial fusion events in live microscopy (Figure 5C and Supplementary movie S4), indicating that flash activity is linked to mitochondrial fusion.

To further explore the link between mitochondrial fusion and pH_{mito} flash propagation, we used fibroblasts (MEFs) from knockout mice that completely lack the endogenous pro-fission protein DRP1 (Ishihara *et al*, 2009) or the inner membrane pro-fusion protein OPA1 (Gomes *et al*, 2011). The size of pH_{mito} flashes increased by ~5-fold in $Drp1^{-/-}$ cells while the area of paGFP regions and the length of the smallest fluorescent objects, an independent readout of mitochondrial length, increased by only ~30% (Figure 6). *Drp1* ablation thus markedly increased the propagation of pH_{mito} flashes without altering their frequency and amplitude (Supplementary Figure S6), consistent with the phenotype of HeLa cells expressing the dominant-negative $DRP1^{K38A}$. In contrast, expression of MFN1 in WT MEFs increased the length of individual mitochondria as expected but did not increase the size of the pH_{mito} flashes or paGFP areas (Figure 6C–E), indicating that enforced fusion of the outer membrane does not promote pH_{mito} flash propagation. Remarkably, *Opa1* ablation abrogated pH_{mito} flash activity (Figure 6C) and $\Delta\Psi_m$ fluctuations (not shown), and reduced as expected both the length of individual mitochondria and the size of paGFP-labelled areas by half (Figure 6D–E). Although $Opa1^{-/-}$ are bioenergetically competent (Gomes *et al*, 2011), not a single pH_{mito} flash was detected in $Opa1^{-/-}$ cells even after application of atractyloside, which increased pH_{mito} flash frequency by four-fold in control cells (Supplementary Figure S6E), or after expression of MFN1, which, as expected, Cipolat *et al* (2004) failed to rescue mitochondrial length and paGFP propagation (Figure 6). Importantly, re-expression of OPA1 restored pH_{mito} flash activity, mitochondrial length, and paGFP matrix propagation to WT levels (Figure 6). These data indicate that OPA1-mediated fusion of the inner membrane, but not MFN1-mediated fusion of the outer membrane, is linked to the pH_{mito} flash activity.

We next tested the impact of OPA1-mediated flash activity on mitochondrial bioenergetics, using ratiometric imaging of TMRM over matrix-targeted GFP to quantify $\Delta\Psi_m$. *Opa1* ablation markedly increased the heterogeneity of $\Delta\Psi_m$ within the mitochondrial population of individual cells (Figure 7A). The $\Delta\Psi_m$ of 2.5-μm^2-wide fluorescent objects had a Gaussian distribution (Figure 7B) whose s.d. increased by 2.5-fold upon *Opa1* ablation, from 10 to 25% (Figure 7C). This indicates that OPA1-mediated fusion promotes the equilibration of mitochondrial membrane potentials. We therefore checked whether this $\Delta\Psi_m$ equilibration was linked to the pH_{mito} flash activity. The distribution of $\Delta\Psi_m$ (measured with TMRM or TMRM/GFP) and of pH_{mito} (measured with SypHer) remained unchanged within the flashing regions (Supplementary Figure S7), indicating that pH_{mito} flashes do not promote energy equilibration within the flashing regions themselves. However, careful analysis revealed that 66% of flashes were associated with hyperpolarization events occurring in adjacent mitochondria (located <2 pixels from a flashing unit). The $\Delta\Psi_m$ changes occurring in these adjacent mitochondria were synchronous but of opposite direction (Figure 7D and Supplementary Movie S5). The hyperpolarization events were not associated with changes in pH_{mito} (Figure 7E) and occurred in ~50% of mitochondria adjacent to a flashing unit (Figure 7F) but never in non-adjacent mitochondria. Importantly, the membrane potentials of the two adjacent mitochondria equilibrated after the event (Figure 7D). On average, the $\Delta\Psi_m$ difference between adjacent mitochondria undergoing opposite changes in membrane potential decreased by ~40% after a flash (Figure 7G). These data show that OPA1-dependent flashes equilibrate the membrane potentials of apposed mitochondria.

Discussion

In this study, we provide several new insights into the mechanism and significance of spontaneous mitochondrial fluctuations. First, we clarify the chemical nature of 'mitochondrial flashes' by using a probe that we show to be responsive to pH but not to superoxide. Superoxide flashes coinciding with $\Delta\Psi_m$ decreases were reported in individual mitochondria from skeletal muscle and intact beating hearts (Wang *et al*, 2008; Pouvreau, 2010; Fang *et al*, 2011; Wei *et al*, 2011), but the cpYFP probe used was shown to be highly sensitive to pH (Schwarzlander *et al*, 2011) and was subsequently used to report matrix alkalinization transients in mitochondria from *Arabidopsis thaliana* root cells (Schwarzlander *et al*, 2012a). The pH/superoxide flashes coincide with $\Delta\Psi_m$ decreases and have similar kinetics and pharmacological profiles, suggesting that they reflect the same bioenergetic event. However, since the two activities were measured with the same cpYFP-based probe reportedly sensitive to both proton and superoxide, the chemical nature of the measured signal is uncertain. By showing that our SypHer probe is insensitive to superoxide, we demonstrate that human mitochondria do in fact transiently alkalinize during decreases in $\Delta\Psi_m$, validating the results obtained in astrocytes (Azarias and Chatton, 2011) and plants (Schwarzlander *et al*, 2012a). The SypHer flashes were altered by increased mitochondrial buffering but not by ROS scavengers and were not associated with fluorescence

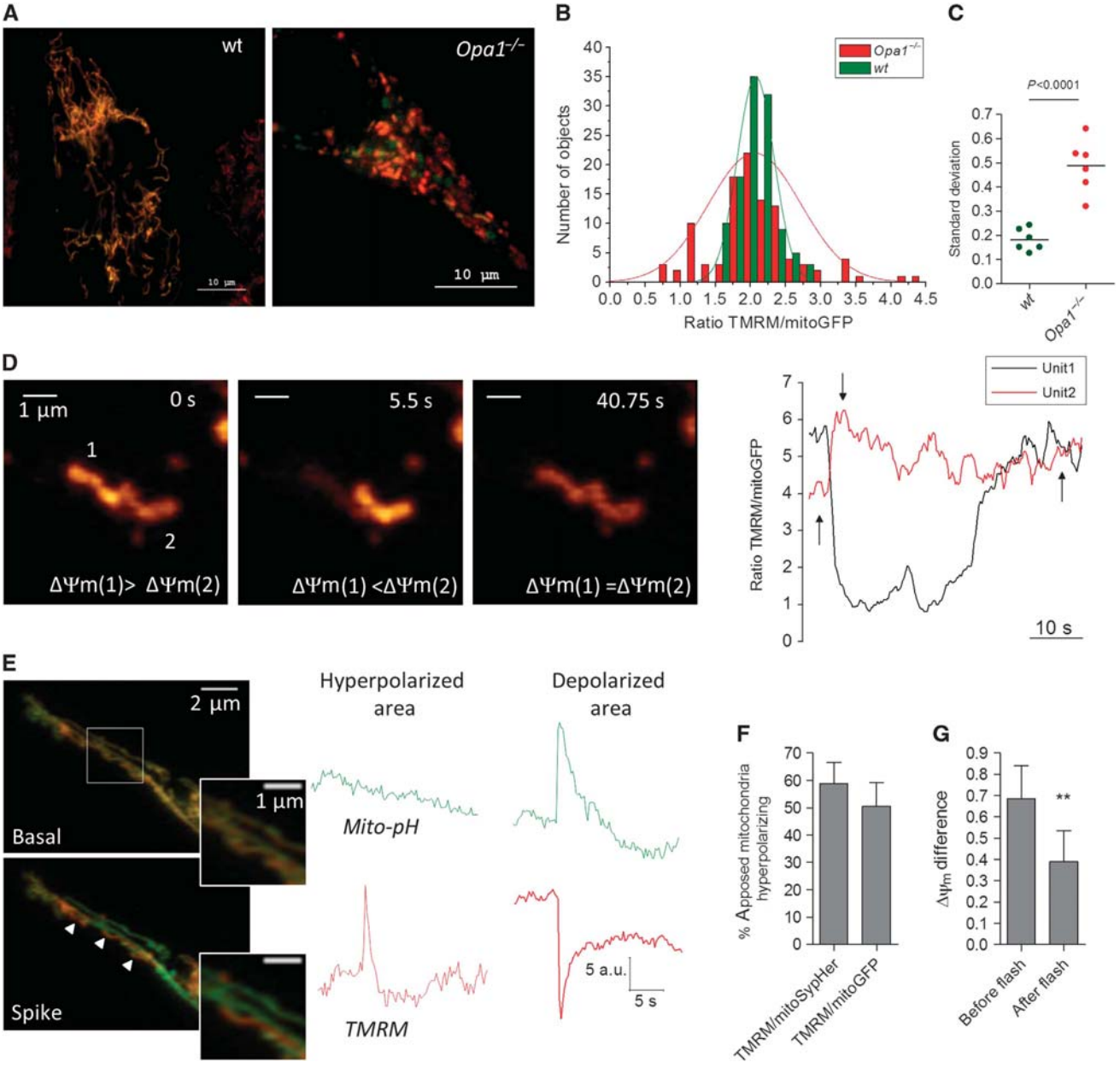

Figure 7 OPA1-mediated pH_{mito} flashes equilibrate the potentials of apposed mitochondria. (**A**) Representative images of wt and *Opa1*$^{-/-}$ MEFs expressing matrix GFP and loaded with TMRM. (**B**) Distribution of $\Delta\Psi_m$ (expressed as TMRM/mitoGFP ratio of 2.5-µm^2-wide fluorescent objects) from these two cells. (**C**) S.d.'s of $\Delta\Psi_m$ Gaussian distributions in mitochondrial populations from six wt and six *Opa1*$^{-/-}$ cells. (**D**) Concomittant hyperpolarization (#1) and depolarization (#2) events in two adjacent mitochondria. Note that the two mitochondrial potentials equilibrated after the event. See Supplementary Movies S5a and S6b. (**E**) $\Delta\Psi_m$ and pH_{mito} recordings of adjacent mitochondria undergoing opposite changes in $\Delta\Psi_m$. The pH_{mito} remained stable in the hyperpolarizing mitochondrion. (**F**) Fraction of adjacent mitochondria (defined as closer than 2 pixels from a flashing mitochondrion) undergoing concomitant hyperpolarization events ($n = 20$–29 cells). (**G**) $\Delta\Psi_m$ difference between adjacent mitochondria measured before and after the synchronous hyperpolarizing/depolarizing event ($n = 23$ events, means ± s.e.m.). $^{**}P < 0.01$.

changes of redox-sensitive green fluorescent protein (roGFP) (data not shown), consistent with protons and not superoxide as the source of the signal. Furthermore, we show that the most potent flash inhibitors, antimycin and CCCP, which are not expected to abrogate superoxide flashes as they increase superoxide production (Muller, 2009), both collapsed ΔpH_m as expected from their pharmacology. Since our probe is insensitive to superoxide, we cannot rule out that superoxide flashes occur concomitantly with pH_{mito} flashes, and this possibility should be evaluated with new probes selective for superoxide and insensitive to pH.

Second, we have causally linked the pH_{mito} flashes to the $\Delta\Psi_m$ decreases by demonstrating that prototypical pH_{mito} flashes can be evoked by artificial depolarization of mitochondria with valinomycin/K^+. In isolated mitochondria equilibrated with valinomycin/K^+, alterations in $\Delta\Psi_m$ are exactly balanced by opposite alterations in ΔpH, and Δp remains constant within a wide range of voltages (Nicholls, 1974; Lambert and Brand, 2004; Nicholls, 2005). We show here that this rule holds true also in permeabilized cells. A transient mitochondrial depolarization thermodynamically favours H^+ extrusion by decreasing the driving force for

proton pumping by respiratory chain complexes, increasing the rate of H^+ extrusion and of O_2 consumption by mitochondria (Nicholls, 1974; Costa *et al*, 1984; Nicolli *et al*, 1991; Talbot *et al*, 2007). The demonstration that this compensatory mechanism occurs spontaneously in intact cells indicates that $\Delta\Psi_m$ fluctuations are not an indicator of mitochondrial dysfunction as concomitant pH_{mito} flashes preserve the proton-motive force, thus maintaining the ability of mitochondria to convert energy. A thermodynamically similar mechanism was recently proposed to account for coincident $\Delta\Psi_m$ and pH_{mito} fluctuations in plant mitochondria, where the pulsing activity was proposed to be triggered by the entry of calcium ions into the matrix (Schwarzlander *et al*, 2012a). In our hands, mitochondrial Ca^{2+} uptake does not appear to trigger pH_{mito} elevations because the spontaneous activity was not altered by Ca^{2+} store depletion, by cytosolic Ca^{2+} chelation (Figure 2), or by knockdown of the mitochondrial H^+/Ca^{2+} exchanger Letm1 (Supplementary Figure S2). By comparing the $\Delta\Psi_m$ and pH_{mito} changes recorded during flashes to the changes evoked by CCCP and oligomycin, we can estimate that $\Delta\Psi_m$ was around -120 mV at rest and decreased to -50 mV during a flash, while pH_{mito} averaged 7.8 at rest and increased by 0.4 pH unit during a flash. The IMS pH was previously measured at 6.8 in HeLa cells (Porcelli *et al*, 2005), and since this parameter strongly depends on proton pumping across the IMS, an acidification of 0.4 pH unit that would match the matrix alkalinization during a flash seems reasonable. We therefore estimate that ΔpH_m is around 1 (-60 mV) at rest and increases to 1.8 (-110 mV) during a flash. Based on these calculations, the resting proton-motive force of -180 mV decreases by only $\sim$20 mV during a flash, but the relative contributions of its electrical and chemical components become inverted.

Third, we show that OPA1-mediated IMM fusion is required for the generation of the coupled $pH_{mito}/\Delta\Psi_m$ fluctuations. $\Delta\Psi_m$ flickers or oscillations were previously linked to mitochondrial Ca^{2+} or Na^+ entry (Duchen *et al*, 1998; De Giorgi *et al*, 2000; Buckman and Reynolds, 2001; Jacobson and Duchen, 2002; Vergun *et al*, 2003; Vergun and Reynolds, 2004; Azarias *et al*, 2008) or attributed to mPTP opening by mitochondria ROS (Huser and Blatter, 1999; De Giorgi *et al*, 2000; Jacobson and Duchen, 2002). We show that pH_{mito} flashes persist in ion-free solutions and are not affected by mPTP inhibitors and ROS scavengers, ruling out cation entry across the mPTP as a trigger of the fluctuations. The unexpected and opposite effects of atractyloside and oligomycin might reflect the diverging effects of these inhibitors on the fusion process. Oligomycin inhibits the ATP synthase while atractyloside inhibits the ANT (Vergun and Reynolds, 2004), causing opposite changes in matrix ATP levels that might differently modulate the formation of a fusion pore. Our observation that the activity disappears in mitochondria lacking the pro-fusion protein OPA1 indicates that the fluctuations are probably linked to the fusion of the mitochondria inner membranes, but this activity differs from the 'kiss-and-run' mode of transient mitochondrial fusion previously reported (Liu *et al*, 2009), which allowed exchange of soluble matrix proteins and promoted mitochondrial mobility. Instead, we propose that the coupled $pH_{mito}/\Delta\Psi_m$ fluctuations reflect the transient openings of a fusion pore between contiguous mitochondria of different membrane potentials (Figure 8). Opening a fusion pore will establish electrical continuity between these mitochondria, decreasing $\Delta\Psi_m$ in the more energized mitochondria. The $\Delta\Psi_m$ decrease will then boost proton pumping by active respiratory chain complexes, generating a pH_{mito} flash in the depolarizing mitochondria. Electrical coupling causes the apposed mitochondria to hyperpolarize during the flash, shutting down proton pumping and preventing pH_{mito} flash propagation in the hyperpolarizing mitochondria. While the existence of pores electrically coupling mitochondria awaits electrophysiological confirmation, our 'junctional coupling' model explains why flash activity is not coupled to ion fluxes and why mitochondria can preserve their bioenergetic competence during the flashes, as connecting two matrixes will not dissipate the proton-motive force. Previous models have implicated the opening of ion channels, transporters, or large conductance pores between the matrix and the IMS/cytosol, processes that have profound impacts on mitochondria bioenergetics and ionic homeostasis. By linking flash activity to OPA1-mediated mitochondrial fusion, a highly regulated cellular process sensitive to calcium elevations and to oxidative stress (Cereghetti *et al*, 2008; Tang *et al*, 2009), our model also accounts for the reported effects of calcium and ROS on flashing activity.

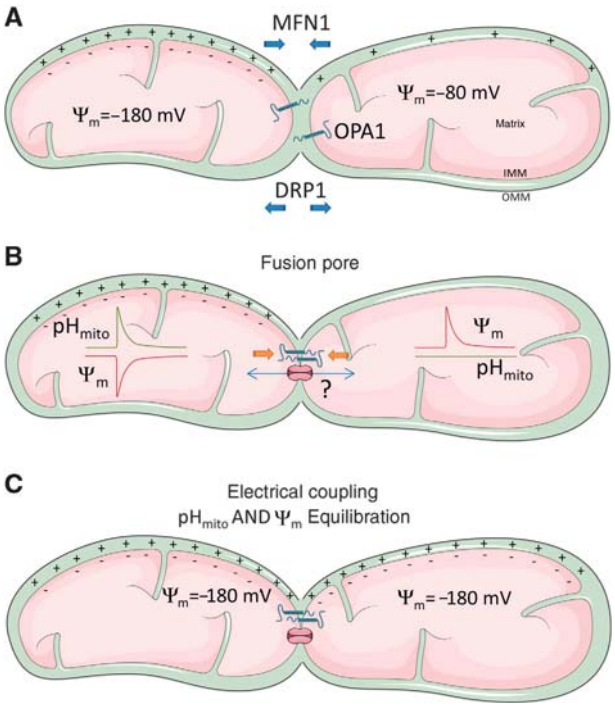

Figure 8 Proposed mechanism of mitochondrial $\Delta\Psi_m/pH_{mito}$ fluctuations. We propose that the $\Delta\Psi_m/pH_{mito}$ fluctuations are triggered by the opening of a fusion pore between two mitochondria of different potential. (**A**) Individual mitochondria can maintain different $\Delta\Psi_m$ and pH_m. (**B**) OPA1-mediated inner membrane fusion leads to the formation of a fusion pore that establishes electrical continuity between adjacent mitochondria, without allowing the diffusion of matrix proteins. The disequilibrium in membrane potentials drags electrons from the more energized mitochondria, causing a decrease in $\Delta\Psi_m$ that boosts proton pumping by the respiratory chain, generating a pH_{mito} flash in the depolarizing mitochondria. Electrical coupling causes the apposed mitochondria to hyperpolarize during the flash, shutting down proton pumping and preventing pH_{mito} flash propagation in the hyperpolarizing mitochondria. (**C**) At the end of the flash, the two interconnected mitochondria are in electrochemical equilibrium.

Finally, our concurrent paGFP and TMRM recordings demonstrate that contiguous mitochondria can synchronize their energetic state without mixing their matrix content. Earlier studies had shown that $\Delta\Psi_m$ flickering could propagate along interconnected mitochondria (De Giorgi *et al*, 2000), but whether $\Delta\Psi_m$ propagation required matrix continuity was not known. Here, we show that inhibition of endogenous DRP1 activity either by genetic ablation or by expression of a dominant-negative mutant greatly enhances the propagation of pH_{mito} elevations along interconnected mitochondria, but marginally increases the propagation of a photoactivated matrix protein. Mitochondrial fusion proceeds unabated in DRP1 incapacitated cells. However, although these mitochondria appear fused on the confocal microscope, their matrix compartments do not allow the free diffusion of matrix paGFP. In contrast, the pH_{mito} fluctuations covered on average 50% of the mitochondrial area and became global in some cells, in which the matrix pH of the whole network increased within 10 ms without any clear initiation spot or visible decay in flash amplitude along labelled structures (Supplementary movie S3). This indicates that the coincident $\Delta\Psi_m/pH_{mito}$ fluctuations propagate by a saltatory mechanism or by a very fast regenerative mechanism. Our observation that $\Delta\Psi_m$ and pH_{mito} rapidly equilibrate along interconnected mitochondria confirms the hypothesis originally formulated by Zorov that $\Delta\Psi_m$ and ΔpH_m immediately spread along mitochondrial inner membranes (Amchenkova *et al*, 1988). We extend this concept by showing that the proton-motive force can equilibrate within milliseconds in contiguous mitochondria that do not mix their matrix protein content. One purpose of mitochondrial fusion is to allow genetic complementation of damaged mitochondrial DNA, but this function requires the mixing of matrix content. We demonstrate that another function of mitochondrial fusion proteins is to electrically couple individual mitochondria in order to synergize their metabolic activity.

In summary, we show here that mitochondria exhibit spontaneous elevations in their matrix pH triggered by bursts of depolarization that both propagate faster than matrix GFP along connected mitochondria. This indicates that mitochondria can be electrically coupled without exchanging their matrix content. We propose that the matrix alkalinization transients reflect increased pumping by the respiratory chain during $\Delta\Psi_m$ decreases triggered by the opening of a fusion pore between neighbouring mitochondria of different membrane potentials. This new mode of mitochondrial coupling might facilitate the transmission of energy inside cells by equilibrating the proton-motive force along electrically connected, but not fused, mitochondria.

Materials and methods

Cell culture and transfection

HeLa cells and 143b cells (*wt* and *Rho 0*) were cultured in Dulbecco's modified Eagle's medium (DMEM) with 1 and 4.5 mg/ml glucose, respectively; WT and *Drp1*$^{-/-}$ MEF cells in DMEM-Glutamax with non-essential amino acids; *Opa1*$^{-/-}$ cells in MEF medium supplemented with uridine (50 μg/ml, Sigma). All media contained 10% FCS, 1% penicillin, and 1% streptomycin. For fluorescence imaging, 10^5 cells were seeded on 25-mm glass cover slips, transfected 24 h later with 2 μg of DNA and 5 μl Lipofectamine 2000, and imaged 48 h later. All reagents were purchased from Invitrogen or Sigma.

Mito-SypHer purification and in vitro characterization

The N-terminal poly-His-tag mito-SypHer was generated by cloning in frame mito-SypHer into the Xho-I/ Hind-III site of the prokaryotes expression vector pBAD/HisB (Invitrogen). TOP10-competent cells (Invitrogen) were transformed and expression induced according to the manufacturer's instructions in the presence of 0.002% arabiniose for 4 h. Cells were lysed and total protein content kept in Tris 25 mM, 150 mM NaCl. After purification in a nickel column, the samples were dialysed at 4°C for 16 h and mito-SypHer concentrated using Amicon Ultra-4 Centrifugal Filter Units (Millipore). Five millimolar β-mercaptoethanol was present throughout the isolation procedures to reduce thiol groups. Twenty microlitre (2 μM) of purified mito-SypHer was dissolved in 200 μl Tris 25 mM, 150 mM NaCl pH 7.5 (0.5 mM β-mercaptoethanol), and fluorescence spectra recorded on a LS50B spectrometer (Perkin Elmer), using 500 μM xanthine and 100 mU XO (Sigma) to generate superoxide.

Superoxide production measurements in vitro

Xanthine (X)/XO O_2^- production was verified by adding 0.01 mM of the luciferin analogue MCLA to a buffer containing 25 mM Tris, 150 mM NaCl, 0.3 mM ethylenediaminetetraacetic acid (EDTA), 0.3 mM β-mercaptoethanol, and 400 μM xanthine (pH 7.5). XO (100 mU) was added to initiate the reaction and the luminescence recorded every 10 s on a FLUOstar (BMG Labtech) microplate reader. To verify the O_2^- specificity of the signal emitted by MCLA, 50 U/ml SOD was included in control experiments.

Mitochondrial pH, $\Delta\Psi_m$, and Ca^{2+} measurements in live cells

Recordings were performed in N-2-hydroxyethylpiperazine-N′-2-ethane sulphonic acid (HEPES) buffer solution containing 140 mM NaCl, 5 mM KCl, 1 mM $MgCl_2$, 2 mM $CaCl_2$, 20 mM HEPES, 10 mM glucose, pH set to 7.4 with NaOH at 37°C. The Ca^{2+}-free solution contained 0.5 mM ethyleneglycol-bis (beta-aminoethylether)-*N*,*N*′-tetraacetic acid (EGTA) and no $CaCl_2$. Mito-SypHer was alternately excited for 200–300 ms at 440 and 488 nm on a Nipkow spinning disk confocal microscope (Visitron Systems GmbH) equipped with a ×63 1.4 NA oil-immersion objective (Carl Zeiss AG). Images were acquired every 800 ms and ratios calculated in MetaFluor 6.3 (Universal Imaging) and analysed in Excel (Microsoft) and GraphPad Prism 5.01 (GraphPad Inc, La Jolla, USA). Mitochondrial pH was calibrated using nigericin (5 μg/ml) and monensin (5 μM) in 125 mM KCl, 20 mM NaCl, 0.5 mM $MgCl_2$, 0.2 mM EGTA, and, Tris (pH 8.0, 9.0), HEPES (pH 7.0–7.5), or MES (pH 5.5–6.5). For each cell, a 5-point calibration curve was fitted to a variable slope sigmoid equation with $1/y$ weighting and constraining the top of the curve to 30 (GraphPad Prism 5.01). For simultaneous pH_{mito}/Ca^{2+}_{mito} measurements, cells were incubated at room temperature for 30 min with 2 μM Rhod-2-AM, washed for 20 min, and imaged immediately. For pH_{mito}/Ψ_m recordings, cells were incubated at room temperature for 20 min with 4 nM TMRM, washed, and kept at 37°C on the microscope until signal reached stability. Mito-SypHer was excited for 300 ms at 488 nm and TMRM or Rhod-2 were excited for 300 ms at 565 nm. Image pairs were acquired every 600 ms.

Measurements in permeabilized cells

Cells were imaged with a ×40, 1.3 NA objective (Zeiss Axiovert s100TV) using a cooled CCD camera (MicroMax, Roper Scientific). For pH imaging, SypHer was alternately excited for 200–300 ms at 430 and 480 nm through a 505DCXR dichroic filter and imaged with a 535DF25 band pass filter (Omega Optical). Cells were permeabilized by a short exposure to digitonin (1 min, 100 μM) in a buffer containing 120 mM KCl, 10 mM NaCl, 1 mM H_2KPO_4, 20 mM HEPES, 5 mM succinic acid, 1 mM ATP-Mg^{2+}, 0.02 mM ADP-K, 1 mM $MgCl_2$, 0.5 mM EGTA adjusted to pH 7.4 with KOH. The ion-free solution contained 10 mM HEPES, 5 mM succinic acid, 0.5 mM EGTA, and sucrose to reach 300 mOsm at pH 7.4. For manipulations of the mitochondrial membrane potential, 1 μM valinomycin was added and sucrose and KCl balanced to reach 300 mOsm at pH 7.4.

Mitochondrial length analysis

Confocal Z-stacks of cells expressing matrix-targeted red fluorescent protein (mtRFP) were acquired on a Nikon 1 AR inverted Microscope using a ×60 objective (oil; CFI Plan APO 1.4 NA) and 561 nm (50 mW) excitation. Analysis of mitochondrial length was performed with Image J tool 'Freehand line selection' by measuring 10 mitochondria per cell (>30 cells per condition; three experiments).

paGFP experiments

Cells transiently expressing paGFP were loaded for 25 min at 37°C with 4 nM TMRM in imaging buffer (135 mM NaCl, 5 mM KCl, 0.4 mM KH_2PO_4, 1 mM $MgSO_4$*$7H_2O$, 20 mM HEPES, 0.1% D-glucose, pH 7.4). Cells with low GFP fluorescence intensity were selected to avoid saturation of the GFP emission upon photoactivation (Patterson and Lippincott-Schwartz, 2002). GFP and TMRM were imaged concurrently on the confocal microscope with the objective described above, using 488 and 561 nm excitation and 520/35 and 624/40 emission filters, respectively. Four images were acquired (one image/second) before applying one single stimulation pulse (500 ms, 405 nm laser, 100% power) followed by live imaging at 1 frame/second for 1 min. Loss of focus and movement artifacts was minimized by using a large pinhole aperture (6.9 AU), the Perfect Focus system (Nikon), and by checking photoactivated areas in ratio images. The NIS Elements AR3.2 software was used for data acquisition and analysis of the area of paGFP detected with 'Auto Detect Area'. Photoactivated areas were measured 5 s after photoactivation to allow paGFP equilibration across the lumen of the mitochondrial network (Twig *et al*, 2006).

Rapid pH and potential measurements

Time-resolved pH and potential imaging was performed on cells transiently transfected with mito-SypHer and loaded with TMRM, using the IMIC Andromeda system (Fondis Electronic) equipped with a ×60 oil objective (UPLAN ×60 oil, 1.35NA, Olympus), 488 and 561 nm lasers for excitation and FF01-446/523/600/677 (Semrock) as emission filter. Two or four binning and cropped sensor mode was used to increase frame rate. The two images were acquired with the same exposure time of 15 ms to obtain acquisition rates of 66 frames per second.

Statistical analysis

All statistical analyses were performed using Prism software (GraphPad). Significance between two sets of experiments was determined using a Student's *t*-test whereas group sets were analysed using ANOVA.

Supplementary data

Supplementary data are available at *The EMBO Journal* Online (http://www.embojournal.org).

Acknowledgements

We thank Prof Claes Wollheim for critical reading of the manuscript, and Mr Cyril Castelbou and Ning Li for expert technical assistance. This work was supported by the Swiss National Foundation grants 310030B-133126 (to ND) and 31003AB_133130 (to LS) and ERC-2011-StG-282280-ERMITO (to LS). JS-D was supported by a fellowship of the Spanish Ministry of Education. The Figure 8 contain illustrations made by Servier Medical Art http://www.servier.fr/servier-medical-art.

Author contributions: JS-D and MG designed and performed experiments, analysed and interpreted data, and contributed to the manuscript. DP and LS designed experiments and contributed to the manuscript. ND conceived the project, designed experiments, analysed data, and wrote the manuscript.

Conflict of interest

The authors declare that they have no conflict of interest.

References

Amchenkova AA, Bakeeva LE, Chentsov YS, Skulachev VP, Zorov DB (1988) Coupling membranes as energy-transmitting cables. I. Filamentous mitochondria in fibroblasts and mitochondrial clusters in cardiomyocytes. *J Cell Biol* **107:** 481–495

Aon MA, Cortassa S, Marban E, O'Rourke B (2003) Synchronized whole cell oscillations in mitochondrial metabolism triggered by a local release of reactive oxygen species in cardiac myocytes. *J Biol Chem* **278:** 44735–44744

Azarias G, Chatton JY (2011) Selective ion changes during spontaneous mitochondrial transients in intact astrocytes. *PloS ONE* **6:** e28505

Azarias G, Van de Ville D, Unser M, Chatton JY (2008) Spontaneous NA+ transients in individual mitochondria of intact astrocytes. *Glia* **56:** 342–353

Ban T, Heymann JA, Song Z, Hinshaw JE, Chan DC (2010) OPA1 disease alleles causing dominant optic atrophy have defects in cardiolipin-stimulated GTP hydrolysis and membrane tubulation. *Hum Mol Genet* **19:** 2113–2122

Bernardi P (1999) Mitochondrial transport of cations: channels, exchangers, and permeability transition. *Physiol Rev* **79:** 1127–1155

Buckman JF, Reynolds IJ (2001) Spontaneous changes in mitochondrial membrane potential in cultured neurons. *J Neurosci* **21:** 5054–5065

Campello S, Scorrano L (2010) Mitochondrial shape changes: orchestrating cell pathophysiology. *EMBO Rep* **11:** 678–684

Cereghetti GM, Stangherlin A, Martins de Brito O, Chang CR, Blackstone C, Bernardi P, Scorrano L (2008) Dephosphorylation by calcineurin regulates translocation of Drp1 to mitochondria. *Proc Natl Acad Sci USA* **105:** 15803–15808

Cipolat S, Martins de Brito O, Dal Zilio B, Scorrano L (2004) OPA1 requires mitofusin 1 to promote mitochondrial fusion. *Proc Natl Acad Sci USA* **101:** 15927–15932

Costa LE, Reynafarje B, Lehninger AL (1984) Stoichiometry of mitochondrial H+ translocation coupled to succinate oxidation at level flow. *J Biol Chem* **259:** 4802–4811

De Giorgi F, Lartigue L, Ichas F (2000) Electrical coupling and plasticity of the mitochondrial network. *Cell Calcium* **28:** 365–370

Duchen MR, Leyssens A, Crompton M (1998) Transient mitochondrial depolarizations reflect focal sarcoplasmic reticular calcium release in single rat cardiomyocytes. *J Cell Biol* **142:** 975–988

Fang H, Chen M, Ding Y, Shang W, Xu J, Zhang X, Zhang W, Li K, Xiao Y, Gao F, Shang S, Li JC, Tian XL, Wang SQ, Zhou J, Weisleder N, Ma J, Ouyang K, Chen J, Wang X *et al.* (2011) Imaging superoxide flash and metabolism-coupled mitochondrial permeability transition in living animals. *Cell Res* **21:** 1295–1304

Frieden M, James D, Castelbou C, Danckaert A, Martinou JC, Demaurex N (2004) Ca(2+) homeostasis during mitochondrial fragmentation and perinuclear clustering induced by hFis1. *J Biol Chem* **279:** 22704–22714

Gomes LC, Di Benedetto G, Scorrano L (2011) During autophagy mitochondria elongate, are spared from degradation and sustain cell viability. *Nat Cell Biol* **13:** 589–598

Guzman JN, Sanchez-Padilla J, Wokosin D, Kondapalli J, Ilijic E, Schumacker PT, Surmeier DJ (2010) Oxidant stress evoked by pacemaking in dopaminergic neurons is attenuated by DJ-1. *Nature* **468:** 696–700

Hattori T, Watanabe K, Uechi Y, Yoshioka H, Ohta Y (2005) Repetitive transient depolarizations of the inner mitochondrial membrane induced by proton pumping. *Biophys J* **88:** 2340–2349

Huser J, Blatter LA (1999) Fluctuations in mitochondrial membrane potential caused by repetitive gating of the permeability transition pore. *Biochem J* **343**(Pt 2): 311–317

Huser J, Rechenmacher CE, Blatter LA (1998) Imaging the permeability pore transition in single mitochondria. *Biophys J* **74:** 2129–2137

Ishihara N, Nomura M, Jofuku A, Kato H, Suzuki SO, Masuda K, Otera H, Nakanishi Y, Nonaka I, Goto Y, Taguchi N, Morinaga H, Maeda M, Takayanagi R, Yokota S, Mihara K (2009) Mitochondrial fission factor Drp1 is essential for embryonic development and synapse formation in mice. *Nat Cell Biol* **11:** 958–966

Jacobson J, Duchen MR (2002) Mitochondrial oxidative stress and cell death in astrocytes–requirement for stored Ca2+ and sustained opening of the permeability transition pore. *J Cell Sci* **115:** 1175–1188

Lambert AJ, Brand MD (2004) Superoxide production by NADH:ubiquinone oxidoreductase (complex I) depends on the pH gradient across the mitochondrial inner membrane. *Biochem J* **382:** 511–517

Liu X, Weaver D, Shirihai O, Hajnoczky G (2009) Mitochondrial 'kiss-and-run': interplay between mitochondrial motility and fusion-fission dynamics. *EMBO J* **28:** 3074–3089

Ma Q, Fang H, Shang W, Liu L, Xu Z, Ye T, Wang X, Zheng M, Chen Q, Cheng H (2011) Superoxide flashes: early mitochondrial signals for oxidative stress-induced apoptosis. *J Biol Chem* **286:** 27573–27581

Muller FL (2009) A critical evaluation of cpYFP as a probe for superoxide. *Free Radic Biol Med* **47:** 1779–1780

Nagai T, Sawano A, Park ES, Miyawaki A (2001) Circularly permuted green fluorescent proteins engineered to sense Ca2 + . *Proc Natl Acad Sci USA* **98:** 3197–3202

Nicholls DG (1974) The influence of respiration and ATP hydrolysis on the proton-electrochemical gradient across the inner membrane of rat-liver mitochondria as determined by ion distribution. *Eur J Biochem* **50:** 305–315

Nicholls DG (2005) Commentary on: 'old and new data, new issues: the mitochondrial Deltapsi' by H. Tedeschi. *Biochimica Et Biophysica Acta* **1710:** 63–65 Discussion 66

Nicolli A, Redetti A, Bernardi P (1991) The K + conductance of the inner mitochondrial membrane. A study of the inducible uniport for monovalent cations. *J Biol Chem* **266:** 9465–9470

Palmer CS, Osellame LD, Laine D, Koutsopoulos OS, Frazier AE, Ryan MT (2011) MiD49 and MiD51, new components of the mitochondrial fission machinery. *EMBO Rep* **12:** 565–573

Patterson GH, Lippincott-Schwartz J (2002) A photoactivatable GFP for selective photolabeling of proteins and cells. *Science* **297:** 1873–1877

Poburko D, Santo-Domingo J, Demaurex N (2011) Dynamic regulation of the mitochondrial proton gradient during cytosolic calcium elevations. *J Biol Chem* **286:** 11672–11684

Porcelli AM, Ghelli A, Zanna C, Pinton P, Rizzuto R, Rugolo M (2005) pH difference across the outer mitochondrial membrane measured with a green fluorescent protein mutant. *Biochem Biophys Res Commun* **326:** 799–804

Pouvreau S (2010) Superoxide flashes in mouse skeletal muscle are produced by discrete arrays of active mitochondria operating coherently. *PloS ONE* **5:** e13035

Santo-Domingo J, Demaurex N (2012) Perspectives on: SGP Symposium on Mitochondrial Physiology and Medicine: the renaissance of mitochondrial pH. *J Gen Physiol* **139:** 415–423

Schwarzlander M, Logan DC, Fricker MD, Sweetlove LJ (2011) The circularly permuted yellow fluorescent protein cpYFP that has been used as a superoxide probe is highly responsive to pH but not superoxide in mitochondria: implications for the existence of superoxide 'flashes'. *Biochem J* **437:** 381–387

Schwarzlander M, Logan DC, Johnston IG, Jones NS, Meyer AJ, Fricker MD, Sweetlove LJ (2012a) Pulsing of membrane potential in individual mitochondria: a stress-induced mechanism to regulate respiratory bioenergetics in Arabidopsis. *Plant Cell* **24:** 1188–1201

Schwarzlander M, Murphy MP, Duchen MR, Logan DC, Fricker MD, Halestrap AP, Muller FL, Rizutto R, Dick TP, Meyer AJ, Sweetlove LJ (2012b) Mitochondrial 'flashes': a radical concept repHined. *Trends Cell Biol* **22:** 503–508

Smirnova E, Griparic L, Shurland DL, van der Bliek AM (2001) Dynamin-related protein Drp1 is required for mitochondrial division in mammalian cells. *Mol Biol Cell* **12:** 2245–2256

Talbot J, Barrett JN, Barrett EF, David G (2007) Stimulation-induced changes in NADH fluorescence and mitochondrial membrane potential in lizard motor nerve terminals. *J Physiol* **579:** 783–798

Tang S, Le PK, Tse S, Wallace DC, Huang T (2009) Heterozygous mutation of Opa1 in *Drosophila* shortens lifespan mediated through increased reactive oxygen species production. *PloS One* **4:** e4492

Thiffault C, Bennett Jr. JP (2005) Cyclical mitochondrial deltapsiM fluctuations linked to electron transport, F0F1 ATP-synthase and mitochondrial Na + /Ca + 2 exchange are reduced in Alzheimer's disease cybrids. *Mitochondrion* **5:** 109–119

Twig G, Graf SA, Wikstrom JD, Mohamed H, Haigh SE, Elorza A, Deutsch M, Zurgil N, Reynolds N, Shirihai OS (2006) Tagging and tracking individual networks within a complex mitochondrial web with photoactivatable GFP. *Am J Physiol Cell Physiol* **291:** C176–C184

Twig G, Hyde B, Shirihai OS (2008) Mitochondrial fusion, fission and autophagy as a quality control axis: the bioenergetic view. *Biochimica Et Biophysica Acta* **1777:** 1092–1097

Uechi Y, Yoshioka H, Morikawa D, Ohta Y (2006) Stability of membrane potential in heart mitochondria: single mitochondrion imaging. *Biochem Biophys Res Commun* **344:** 1094–1101

Vergun O, Reynolds IJ (2004) Fluctuations in mitochondrial membrane potential in single isolated brain mitochondria: modulation by adenine nucleotides and Ca2 + . *Biophys J* **87:** 3585–3593

Vergun O, Votyakova TV, Reynolds IJ (2003) Spontaneous changes in mitochondrial membrane potential in single isolated brain mitochondria. *Biophys J* **85:** 3358–3366

Wang W, Fang H, Groom L, Cheng A, Zhang W, Liu J, Wang X, Li K, Han P, Zheng M, Yin J, Mattson MP, Kao JP, Lakatta EG, Sheu SS, Ouyang K, Chen J, Dirksen RT, Cheng H (2008) Superoxide flashes in single mitochondria. *Cell* **134:** 279–290

Wei L, Salahura G, Boncompagni S, Kasischke KA, Protasi F, Sheu SS, Dirksen RT (2011) Mitochondrial superoxide flashes: metabolic biomarkers of skeletal muscle activity and disease. *FASEB J* **25:** 3068–3078

Zorov DB, Filburn CR, Klotz LO, Zweier JL, Sollott SJ (2000) Reactive oxygen species (ROS)-induced ROS release: a new phenomenon accompanying induction of the mitochondrial permeability transition in cardiac myocytes. *J Exp Med* **192:** 1001–1014

